# Correlation effects in the electronic structure and photoemission spectra of mixed-valence cerium compounds

Atsushi Fujimori
*Laboratorium für Festkörperphysik, Eidgenössische Technische Hochschule, Hönggerberg, CH-8093 Zürich, Switzerland*
*and National Institute for Research in Inorganic Materials, Sakura-mura, Niihari-gun, Ibaraki 305, Japan**
(Received 2 June 1983)

The electronic ground states and core-hole and valence-hole excited states of so-called tetravalent and mixed-valence Ce compounds are studied taking into account strong correlations among $4f$ electrons. By an analysis of the core-level photoemission satellites, $CeO_2$, which has been thought to be tetravalent, is identified as a mixed-valence system with $\sim 0.6$ $4f$ electron, where the magnetic moment of the $4f^1$ configuration is quenched via singlet coupling between the $4f$ electron and the O $2p$ hole. $4f$-derived satellite features in the resonant photoemission spectrum of $CeO_2$ are calculated, which qualitatively explain resonant photoemission spectra of tetravalent Ce intermetallic compounds. The core-level and $4f$-derived photoemission spectra of mixed-valence CeN are also studied by considering only the $4f$-electron—N $2p$-hole coupling as in $CeO_2$ and neglecting the $4f$-$5d$ mixing. It is also suggested that for the $\alpha$ phase of Ce metal the absence of a localized magnetic moment, volume collapse, and a $4f^0$ signal in the core-level photoemission spectra are explained by this type of configuration-mixing description.

## I. INTRODUCTION

There has been much controversy on the nature of the $4f$ state in Ce compounds, to which a variety of anomalous physical and chemical properties have been ascribed.[1] A central issue is the $\gamma$- to $\alpha$-phase transition in Ce metal, where the localized magnetic moment of the Ce $4f^1$ configuration disappears and the lattice volume decreases by $\sim 15\%$ in going from the $\gamma$ to $\alpha$ phase. Absence of a localized magnetic moment and small lattice volume are also seen in so-called tetravalent Ce compounds and at least at low temperatures in mixed-valence Ce compounds. This fact might suggest that common mechanisms are responsible for the above properties in all these compounds, although quite different $4f$-electron numbers have generally been supposed: $\alpha$-Ce has nearly one $4f$ electron[2–8] as in $\gamma$-Ce, mixed-valence Ce compounds have a nonintegral $4f$ number between zero and 1, and tetravalent compounds have no $4f$ electron.

Recently, fundamental questions have been raised against the existence of purely tetravalent ($4f^0$) Ce compounds by x-ray absorption and photoemission spectroscopies. The x-ray absorption edge of all tetravalent Ce compounds studied by Bauchspiess *et al.*[9] including $CeO_2$ has shown both trivalent and tetravalent features. Some authors[10,11] have attributed these features to final-state effects due to strong perturbation by a core hole, namely $4f^0 \rightarrow 4f^1$ transition. However, for $CeRu_2$, $CeCo_2$, $CeRh_3$, etc., which are nonmagnetic and have also been thought to be tetravalent, $4f$-derived emission was observed by resonant photoemission.[12–14] Core-level x-ray photoemission spectroscopy (XPS) of these compounds has shown both $4f^1$ and $4f^0$ lines.[10] Therefore, if the $4f^1$ features in the core-level spectra are largely due to the initial-state $4f^1$ component rather than to the final-state effects, the tetravalent compounds should be regarded as mixed valence and certain properties of mixed-valence and tetravalent compounds would be explained on the same basis.

In the present paper, photoemission spectra of some nonmagnetic Ce compounds are studied theoretically in order to quantitatively investigate the electronic structure of these compounds, e.g., the $4f$-electron number. Electron correlations among the $4f$ electrons are explicitly taken into account in the initial state as well as in the final state of photoemission. A mechanism is proposed in which a localized magnetic moment of Ce $4f$ can be quenched via hybridization with neighboring orbitals. This hybridization can give any $4f$ number between 0 and 1 depending on materials, and it is strongly suggested that a significant amount of the $4f$ electron is present in all tetravalent Ce compounds.

First, we consider a typical tetravalent oxide $CeO_2$ which is nonmagnetic[15] and insulating, and can be most simply understood as the $4f^0$ configuration and the completely filled O $2p$ valence band. We shall show, however, in the following sections that the ground state of $CeO_2$ is a mixture of the $4f^0$ and $4f^1$ configurations. The core-level XPS of $CeO_2$ as well as other tetravalent compounds[16] [$Ce(tmhd)_4$ (tmhd = tetramethylheptane dionato), $BaCeO_3$] exhibits quite different features from those of trivalent ($4f^1$) compounds. The core-level spectra of trivalent compounds show main $4f^1$ and weaker $4f^2$ shake-down peaks, both originating from the stable $4f^1$ initial-state configuration. The energy separation between the $4f^1$ and $4f^2$ peaks is 2—6 eV, and in general the satellite intensity decreases rapidly with increasing peak

 ©1983 The American Physical Society

separation.[17] In $CeO_2$, on the other hand, two intense peaks separated by as much as $\sim 16$ eV are observed together with weaker peaks at the higher-binding-energy side of the low-energy intense peak (Fig. 1). Burroughs *et al.*,[16] based on the $4f^0$ ground state, have identified the highest-binding-energy peak with the main line ($4f^0$ final state) and the lowest-binding-energy peak with a ligand-to-$4f$ shake-down satellite ($4f^1$ final state), but according to Ref. 17 (hereafter referred to as I) such a high intensity would not be expected for that large a main-satellite separation. Furthermore, the weak lines could not be given a reasonable assignment.

A recent theoretical study using the scattered-wave—$X\alpha$ (SW-$X\alpha$) method for a $CeO_8$ cluster[18] has identified the lowest-binding-energy peak as the main peak and the weak lines as ligand-to-$4f$ shake-up satellites. These authors, however, could not give a reasonable explanation for the intense highest-binding-energy peak, and tentatively attributed it to the Ce $5p$-to-$np$ transition. The latter assignment is hardly acceptable because one would expect similar transitions in $Ce_2O_3$ or in $La_2O_3$ which have not been observed. Basic difficulty probably lies in an assignment based on one-electron molecular-orbital energy diagrams in terms of which one cannot properly take into account electron correlations among the $4f$ electrons, in particular in the final state of photoemission. It has been found in some cases even in correlated systems that one-electron theories give correct ground-state properties such as total energies, electron distribution, magnetization, etc.[8,19]; in fact, in the SW-$X\alpha$ study[18] the $4f$ occupancy in the ground state has been calculated to be $\sim 0.5$, which is in fair agreement with our present results. However, the success of one-electron theories only means that the above quantities are well approximated by expectation values of a single Slater determinant consisting of molecular orbitals, but does not necessarily mean that the real ground-state wave function itself is properly represented by the single Slater determinant.

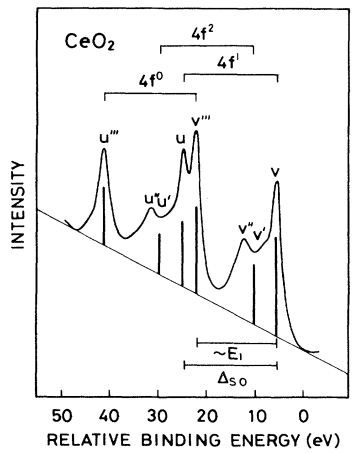


FIG. 1. Experimental (Ref. 16) and calculated Ce $3d$ core-level XPS spectra of $CeO_2$. $v$, $v'$, $v''$, and $v'''$ belong to the Ce $3d_{5/2}$ spin-orbit component and $u$, $u'$, $u''$, and $u'''$ to the Ce $3d_{3/2}$ component. The calculated spectrum is shown by vertical bars. $4f^0$, $4f^1$, and $4f^2$ represent main components of the final states. $E_1 = E'(4f^0 \rightarrow 4f^1 L^{-1})$ is an energy required to move an electron from O $2p$ to Ce $4f$ in the presence of the core hole and $\Delta_{so}$ is the spin-orbit splitting between the $3d_{5/2}$ and $3d_{3/2}$ levels.

We therefore use a basis set with the definite numbers of the $4f$ electrons, which is suited for strongly correlated systems. When the initial state is a mixture of the $4f^0$ and $4f^1$ configurations, the core-level spectra show characteristics of valence mixing, namely $4f^0$, $4f^1$, and $4f^2$ final-state peaks. In this case the $4f^0$ peak as well as the $4f^1$ peak mainly arises from a direct transition, not by a shake-up or shake-down process, and therefore can be intense irrespective of the $4f^0$-$4f^1$ line separation. This configuration mixing in $CeO_2$ is of a local type $4f^0 \leftrightarrow 4f^1 L^{-1}$, where $L^{-1}$ is a ligand (O $2p$) hole, and does not necessarily imply the position of the $4f$ level located at the Fermi level $E_F$ as in the usual valence-mixing mechanism involving conduction electrons $4f^0(5d6s)^n \leftrightarrow 4f^1(5d6s)^{n-1}$, where $(5d6s)^n$ represents $n$ electrons in the $5d6s$ conduction band. The $4f$ occupancy is thus obtained to be as large as $\sim 0.6$.

We also present the $4f$-derived emission spectrum of $CeO_2$ which can be observed in resonant photoemission spectroscopy. It is shown that gross features of the $4f$ spectrum of tetravalent Ce compounds are not very different from those of trivalent compounds studied in I. This would account for the $4f$ emission from tetravalent $CeRu_2$, $CeCo_2$, $CeRh_3$, etc.,[12–14] similar to those of trivalent $CeAl_2$, $\gamma$-Ce, etc.[20,21]

The local valence mixing $4f^0 \leftrightarrow 4f^1 L^{-1}$ as well as extended $4f^0(5d6s)^n \leftrightarrow 4f^1(5d6s)^{n-1}$ might be important in metallic mixed-valence systems such as CeN,[22] $CePd_3$,[23,24] etc. Thus we have applied the above procedure to CeN by neglecting interactions between the $4f$ level and the $5d$ conduction band. The results reproduce well the core-level XPS (Ref. 25) and resonant photoemission[26] spectra with the $4f$ occupancy of $\sim 0.8$, which is considerably larger than previously accepted values estimated from the lattice volume,[22,27] although the $4f^0(5d6s)^n \leftrightarrow 4f^1(5d6s)^{n-1}$ mixing is also suggested to be significant.

The same mixed-valence mechanism as in $CeO_2$ could also be responsible for the $\alpha$ phase of Ce metal, where the localized magnetic moment of Ce $4f$ disappears. The core-level XPS spectra of $\alpha$-Ce have clearly shown $4f^0$ final-state signals.[25,28] This fact indicates that the $4f^0$ component, though much smaller than in $CeO_2$, is present in the ground state of $\alpha$-Ce. It should be noted that an essential point is the symmetry of the $4f$ state but is not the $4f$ occupancy. A simplified model is presented for the $\gamma$-to-$\alpha$ transition and discussed with relation to the resonant photoemission below.

The organization of this paper is as follows: In Sec. II general discussion of core-level and $4f$-derived resonant photoemission spectra are given for stable trivalent and tetravalent or mixed-valence Ce compounds. In Sec. III formulation based on a cluster model is developed with $CeO_2$ as an example. Results for $CeO_2$ and CeN are given in Secs. IV and V, respectively. A model for the $\gamma$-to-$\alpha$ transition of Ce metal is presented in Sec. VI. Finally, in Sec. VII, relation of our model to other mixed-valence descriptions are discussed. A summary of the results for $CeO_2$ has already been published elsewhere.[29]

## II. GENERAL DESCRIPTION OF CORE-LEVEL AND 4f-DERIVED PHOTOEMISSION

Photoemission spectroscopy is a powerful tool in studying mixed-valence systems: Although a photoinduced hole produces strong perturbations in the system studied, spectroscopic selection rules would give unique opportunity to characterize the electronic structure of the ground state. Before proceeding with mathematical formulation, we describe a general picture of the core-level and resonant $4f$ photoemission for mixed-valence Ce compounds. In the sudden approximation the intensity of an XPS core level is given by

$$I_F \propto |\langle \Psi_I' | \Psi_F' \rangle|^2 , \tag{1}$$

where $\Psi_F'$ is a core-hole final state and $\Psi_I'$ is a core-hole state with all other orbitals frozen in the initial state. Equation (1) means that the intensity of a final state is determined by a projection of the initial state onto the final state. As has been shown in I, for stable-valence (Ce $4f^1$) compounds there is hybridization among different final-state configurations which give rise to so-called shake-up or shake-down transitions. For mixed-valence compounds hybridization both in the initial and final states should be considered. The degree of hybridization is generally large between those two configurations which are close to each other in energies. Figure 2 illustrates transitions associated with a core-level ionization. There intensities of transitions are designated by thickness of arrows and resulting spectra are also schematically shown: In the $4f^1$ compound the ground state is almost purely $4f^1$, while in the mixed-valence compound the initial state is a mixture of the $4f^0$ and $4f^1$ configurations and the $4f^0$ signal is intense owing to the direct transition from the initial-state $4f^0$ component.

In resonant photoemission a photon is resonantly absorbed, $4d^{10}4f^1+h\nu \rightarrow 4d^9 4f^2$, and then the $4d^9 4f^2$ state decays via a super-Coster-Kronig (SCK) decay into $4d^{10}4f^0+\epsilon l$. As the intermediate state is localized due to the strong core-hole potential, a localized $4f^0$ hole is left in the final state. Thus the $4d \rightarrow 4f$ resonant photoemission can be described simply as enhanced $4f$ emission of the $4f$ electron, that is, the intensity is effectively given by

$$I_F \propto |\langle \Psi_I | e\vec{r} | \Psi_F \rangle|^2 , \tag{2}$$

where dipole matrix elements for the $4f$-emission ($4f^1 \rightarrow 4f^0$) component are predominant. As can be seen in Fig. 3, $4f^1$ and mixed-valence Ce compounds show grossly similar spectra: Two features corresponding to the $4f^0$ and $4f^1$ final states are expected, the latter being allowed by hybridization with the former state.

## III. GROUND STATE, CORE-HOLE, AND VALENCE-HOLE STATES OF THE Ce-LIGAND CLUSTER

We describe in this section theoretical details by using $CeO_2$ as an example. $CeO_2$ forms in the $CaF_2$ structure as in Fig. 4. As we are interested only in localized excitations, a $CeO_8^{12-}$ cluster as in the figure is considered. The present formulation is closely related to that in I, where we have studied stable-valence cerium with the ground state having a localized magnetic moment of $4f^1(^2F_{5/2})$, while here the ground state is nonmagnetic and therefore should be fully symmetric (singlet) with respect to both orbitals and spins. In addition to an obvious singlet configuration, $4f^0$ configuration with the com-

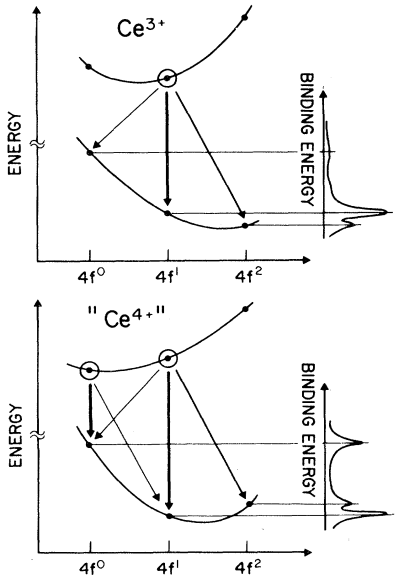


FIG. 2. Energy diagrams for core-level photoemission from trivalent ($Ce^{3+}$) and tetravalent ($Ce^{4+}$) or mixed-valence Ce. Intensities of the transitions are given by thickness of arrows. Resulting spectra are shown on the right-hand side.

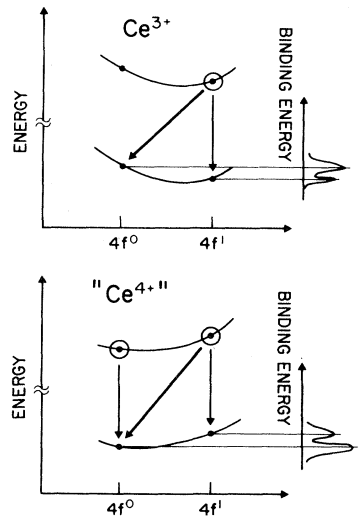


FIG. 3. Energy diagrams for $4f$-derived photoemission from trivalent ($Ce^{3+}$) and tetravalent ($Ce^{4+}$) or mixed-valence Ce. Resulting spectra are shown on the right-hand side.

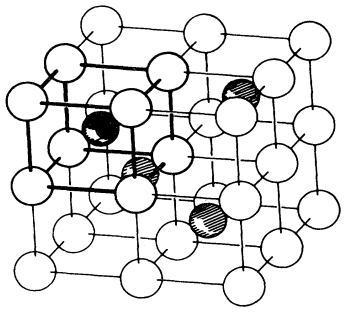

FIG. 4. Crystal structure of $CeO_2$. Open and shaded circles represent O and Ce atoms, respectively. The $CeO_8$ cluster used in the present study is indicated by thick lines.

pletely filled O $2p$ levels, we can also consider a $4f^1$—ligand-hole ($4f^1L^{-1}$) complex having the full symmetry of the cluster. As the $4f^1L^{-1}$ configuration is expected to lie not too high in energy as compared to the $4f$-$L$ hybridization ($\sim 1$ eV), the mixing $4f^0 \leftrightarrow 4f^1L^{-1}$ must be present. The ground state may thus be written as

$$\Psi_I = c_{I0}\,|\,0\rangle + \sum_l c_{Il}\,|\,l\rangle \ , \tag{3}$$

$$|\,l\rangle = \alpha_l^\dagger\,|\,0\rangle = \sum_{i,j}\Gamma_{ij}^l \sum_\sigma L_{i\sigma} f_{j\sigma}^\dagger\,|\,0\rangle \ , \tag{4}$$

where $L_{i\sigma}$ and $f_{j\sigma}^\dagger$ are operators which annihilate an electron in a ligand level $L_i$ and create an electron in a $4f$ crystal-field level $f_j$ with spin $\sigma$, respectively. The first term $|\,0\rangle$ represents the $4f^0$ configuration with the closed O $2p$ shell (to be exact, the completely filled Ce $5d$—O $2p$ bonding levels) and the second term represents the $4f^1$ state where the $4f$ electron and ligand hole form a singlet state. The coefficients $\Gamma_{ij}^l$'s are to make the ground state fully symmetric. Within the $CeO_8$ cluster model we have four $l$'s in (3), two of which involve $t_{1u}$-like molecular orbitals, one of which is $t_{2u}$-like and the rest are $a_{2u}$-like orbitals.

The ground state is obtained by solving a secular equation

$$\sum_m H_{lm}c_{Im} = E_I c_{Il} \ . \tag{5}$$

Nonzero matrix elements of the Hamiltonian in (5) have the form of $H_{0l} = \langle 0\,|\,H\,|\,l\rangle = V_l$ and $H_{ll} = \langle l\,|\,H\,|\,l\rangle = E(4f^0 \rightarrow 4f_i L_j^{-1})$, which is an energy required to move an electron from $L_j$ to $4f_i$ in the orbital set $l$. According to the SW-$X\alpha$ results[18] two $V_l$'s out of four are significant, one involving $a_{2u}$-like orbitals and the other involving $t_{1u}$-like orbitals, and we retain only the two $V_l$'s. Moreover, we set $E(4f^0 \rightarrow 4f_i L_j^{-1})$'s for $a_{2u}$ and $t_{1u}$ to be the same (equal to $E_0$) since the ligand orbitals $a_{2u}$ and $t_{1u}$ have the same energies within 0.01 Ry.[18] Thus the Hamiltonian is

$$\begin{bmatrix} 0 & V_1 & V_2 \\ V_1 & E_0 & 0 \\ V_2 & 0 & E_0 \end{bmatrix} . \tag{6}$$

Transfer integrals $\langle f_{xyz}\,|\,h\,|\,L_{xyz}\rangle$ for $a_{2u}$ and $\langle f_x\,|\,h\,|\,L_x\rangle$ for $t_{1u}$, where $h$ is the one-electron Hamiltonian, are estimated from the energy-level diagram and the $4f$ populations of the $CeO_8$ cluster[18] to be 1.05 and 0.70 eV, respectively. Then using relations

$$|\,t_{1u}\rangle = (1/\sqrt{2})[(1/\sqrt{3})(L_{x\uparrow}f_{x\uparrow}^\dagger + L_{y\uparrow}f_{y\uparrow}^\dagger + L_{z\uparrow}f_{z\uparrow}^\dagger) + (\downarrow \text{ terms})]\,|\,0\rangle \ ,$$

$$|\,a_{2u}\rangle = (1/\sqrt{2})[L_{xyz\uparrow}f_{xyz\uparrow}^\dagger + (\downarrow \text{ term})]\,|\,0\rangle \ ,$$

we obtain $V_1 = \sqrt{2}\langle f_{xyz}\,|\,h\,|\,L_{xyz}\rangle = 1.48$ eV and $V_2 = \sqrt{6}\langle f_x\,|\,h\,|\,L_x\rangle = 1.71$ eV.

Valence electrons in a core-hole state are also in a singlet state if one can neglect the core-hole—$4f$-multiplet coupling. This would be a good approximation for the $3d$ core levels which we are going to treat here. Thus the core-hole state is given by

$$\Psi_F' = c_{F0}\,|\,0'\rangle + \sum_l c_{Fl}\,|\,l'\rangle + \sum_{l,m} c_{Flm}\,|\,lm'\rangle \ , \tag{7}$$

$$|\,l'\rangle = \alpha_l^\dagger\,|\,0'\rangle \ , \tag{8}$$

$$|\,l,m'\rangle = \alpha_l^\dagger\alpha_m^\dagger\,|\,0'\rangle \ , \tag{9}$$

where primes represent the presence of a core hole on Ce. The first, second, and last terms in (7) represent, respectively, the $4f^0$, $4f^1$, and $4f^2$ final states. Within the same approximation as that for the initial state we use two $V_l$'s in the second term and one ($l = t_{1u}$ and $m = a_{2u}$) in the last term of (7). Thus the final-state Hamiltonian is

$$\begin{bmatrix} 0 & V_1 & V_2 & 0 \\ V_1 & E_1 & 0 & V_2 \\ V_2 & 0 & E_1 & V_1 \\ 0 & V_2 & V_1 & E_1+E_2 \end{bmatrix} . \tag{10}$$

Here $E_1 = E'(4f^0 \rightarrow 4f^1L^{-1})$ is an energy required to move an electron from the ligand to $4f$ level, and $E_2 = E'(4f^1L^{-1} \rightarrow 4f^2L^{-2})$ is that required to further move one more electron in the presence of the core hole. The intensity of the final state $\Psi_F'$ is given within the sudden approximation by

$$I_F \propto \left| c_{F0}c_{I0} + \sum_l c_{Fl}c_{Il} \right|^2 . \tag{11}$$

The valence-band spectrum is obtained by considering a valence-hole state

$$I_{fi\sigma} = c_{F0}L_{i\sigma}\,|\,0\rangle + \sum_l c_{Fl}L_{i\sigma}\,|\,l\rangle \ . \tag{12}$$

One can see that (12) consists of one-ligand-hole and two-ligand-hole—one-$4f$-electron parts. Again we consider only valence-hole states with the $a_{2u}$ and $t_{1u}$ symmetry because here we are interested only in $4f$-derived photoemission which arises from the second term of the initial state (3) involving only ligand holes with $a_{2u}$ and $t_{1u}$ characters. Emission from ligand orbitals which do not couple with Ce $4fa_{2u}$ or $t_{1u}$ gives simply one-electron density-of-states (DOS) features of occupied molecular orbitals. For the

$a_{2u}$-hole state or the $t_{1u}$-hole state we solve the secular equation of the Hamiltonian

$$\begin{bmatrix} \epsilon_L & \bar{V}_1 & \bar{V}_2 \\ \bar{V}_1 & \epsilon_L + E_a & 0 \\ \bar{V}_2 & 0 & \epsilon_L + E_a \end{bmatrix}, \tag{13}$$

where $\epsilon_L$ is the O $2p$ level energy and $E_a = E(4f^0L^{-1} \rightarrow 4f^1L^{-2})$. For the $a_{2u}$-like hole state [i.e., $i = a_{2u}$ in (12)] $\bar{V}_1 = (1\sqrt{2})V_1$ because of the Pauli principle and $\bar{V}_2 = V_2$. For the $t_{1u}$-like hole state [i.e., $i = t_{1u}x$, $y$, or $z$ in (12)] $\bar{V}_1 = V_1$ and $\bar{V}_2 = \sqrt{5/6}V_2$. Note that the energy zero of (13) is the initial ground state. Thus the intensity of resonant photoemission appearing at a binding energy $E_B$, an eigenvalue of (13), is given by

$$I_{Fi} \propto |c_{F0}c_{Ii}|^2, \tag{14}$$

for the $i\sigma$-hole final state, where $i = a_{2u}$, $t_{1u}x$, $y$, or $z$.

## IV. $CeO_2$

The XPS spectrum of the Ce $3d$ core level in $CeO_2$ consists of two spin-orbit components $3d_{5/2}$ and $3d_{3/2}$ separated by $\sim 20$ eV, each having satellite structures as are described in Sec. I (Fig. 1). The Ce $4d$ spectrum shows also similar satellite structures,[16] though spin-orbit splitting is much smaller and multiplet splittings are significant. The parameters $E_0$, $E_1$, and $E_2$ have been adjusted to reproduce the experimental spectrum: $E_0 = 0.1$, $E_1 = -14.2$, and $E_2 = 1.1$ eV; $\Delta_{so} = 19.5$ eV has been used. The signal $u'''$ ($v'''$) corresponds to the $4f^0$ final state arising mostly from the initial-state $4f^0$ component (see Fig. 2). $u$ ($v$) is the $4f^1$ final state arising from the $4f^1$ initial state, and $u'$ and $u''$ ($v'$ and $v''$) are the $4f^2$ final states resulting from $L$-to-$4f$ shake-up transitions from the $4f^1$ final states. The $4f$ occupancy thus obtained is $\sim 0.6$ (Table I), which agrees well with that obtained by the x-ray absorption edge, 0.68.[9]

$4f$-derived emission using the above parameters are shown as a function of $E_a$ in Fig. 5. Stronger lines are due to $4f$ emission leaving a $4f^0L^{-1}$ state, while weaker features are due to $4f^1L^{-2}$-dominant final states arising from $4f$ emission followed by the $L \rightarrow 4f$ transition. So far resonant photoemission of $CeO_2$ has not been reported. The valence-band XPS spectrum of $CeO_2$ (Ref. 30) seems to be consistent with $4f$ emission overlapping the O $2p$ emission, as the O $2p$-band width appears a little larger than that of $La_2O_3$. This might correspond to the calculated spectrum of $E_a = 1$–$2$ eV in Fig. 5, where $4f$ emission overlaps the O $2p$ band.

TABLE I. Energies (in eV) and $4f^0$ and $4f^1$ population of the ground state and singlet excited states of the $CeO_8^{12-}$ cluster.

| Energy[a] | $4f^0$ | $4f^1$ ($a_{2u}$) | $4f^1$ ($t_{1u}$) |
|---|---|---|---|
| −2.21 | 0.39 | 0.44 | 0.17 |
| 0.10 | 0.28 | 0.56 | 0.16 |
| 2.31 | 0.32 | 0.00 | 0.68 |

[a]Pure $4f^0$ state is taken as the energy zero.

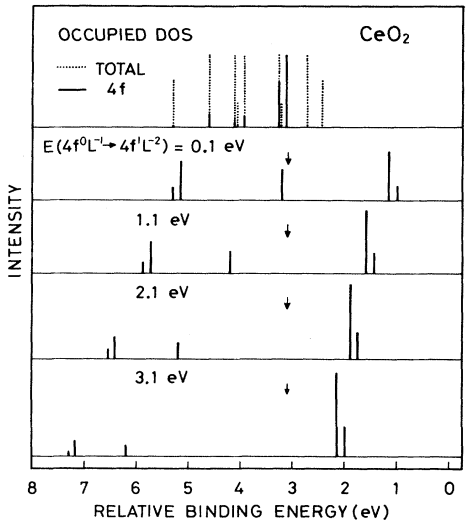


FIG. 5. Calculated $4f$-derived photoemission spectra of $CeO_2$ as a function of $E_a = E(4f^0L^{-1} \rightarrow 4f^1L^{-2})$. The O $2p$ ($a_{2u}$ and $t_{1u}$) level (equal to $\epsilon_L$) is shown by arrows. The top panel shows the one-electron density of states of the $CeO_8$ cluster (Ref. 18).

The $4f$ spectra in Fig. 4 would explain gross features of the $4f$-derived emission in the tetravalent compounds $CeRu_2$, $CeCo_2$, and $CeRh_3$.[12–14] This may give evidence that they are mixed valence rather than $4f^0$. Furthermore, the intensities of the $4f^0$, $4f^1$, and $4f^2$ core-level lines[10] suggest that the $4f$ occupancy in these compounds are closer to 1 rather than to 0.

We compare here the present results with those of the SW-$X\alpha$ calculation.[18] In SW-$X\alpha$ cluster calculations the ground state of a core-ionized state is assigned to the main line and excited states to shake-up states. This has sometimes caused confusion, particularly in cases where the ground state of a core-hole state is reached by a shake-down transition. It should be noted, however, that both in SW-$X\alpha$ and other theories the core hole is generally most effectively screened in the lowest-binding-energy core-hole state.[31] In the case of $CeO_2$, the core-hole ground state in the SW-$X\alpha$ calculation corresponds to one ($4f^1$) of the two ($4f^0$ and $4f^1$) main lines, and the shake-up satellites in the SW-$X\alpha$ results also correspond to the $4f^2$ final states arising from the $L$-to-$4f$ shake-up transitions. In the SW-$X\alpha$ ground state the $4f$ occupancy has been calculated to be about 0.45 within the Ce muffin-tin sphere, which is well compared with our result $\sim 0.6$. It seems that one-electron local-density calculations usually give reasonable $4f$-electron numbers in the ground state if the calculation is performed to self-consistency.[8,19] In fact, in the $3d$ core-hole ground state the $4f$ number increases to about 0.9 and in the shake-up states further to $\sim 1.3$, which corresponds well to our $4f^1$ and $4f^2$ final states. The SW-$X\alpha$ shake-up energies, however, are too small ($\sim 2$ eV) in the SW-$X\alpha$ results as compared to the experimental ones ($\sim 5$ eV). This discrepancy is inherent in the SW-$X\alpha$ method itself, and is not discussed further here. The basic difficulty in the SW-$X\alpha$ calculation is that it could not explain the $4f^0$ final-state lines ($u'''$ and $v'''$).

These final states would probably not be reached by a one-electron excitation from the core-hole ground state but would essentially need a many-electron excitation in the molecular-orbital picture. The use of the basis set with the definite numbers of the $4f$ electron instead of molecular-orbital bases is therefore quite suitable in describing such a strongly correlated system.

We note that some characteristic features of mixed-valence Ce compounds, e.g., disappearance of a localized magnetic moment, small lattice volume could be understood within the present model. As the ground state (3) is a bonding state between the $4f^0$ and $4f^1L^{-1}$ configurations, it is stabilized for a smaller lattice volume through increased $4f$-ligand hybridization as compared to the nonbonding localized $4f^1$ state. Stabilization energy in $CeO_2$ relative to the pure $4f^0$ configuration is 2.2 eV as in Table I. We may infer that the anomalous magnetic behavior of mixed-valence Ce are largely due to low-lying magnetic excited states of the $4f$ ion rather than from the ground state itself. In the case of $CeO_2$, $4f^1L^{-1}$ states, which could be magnetic, have been calculated to be $\sim 2.3$ eV above the ground state and in fact no anomalous magnetism has been observed experimentally.[15]

The parameters for the core-hole state obtained here, $E'(4f^0 \rightarrow 4f^1L^{-1})$ and $E'(4f^1L^{-1} \rightarrow 4f^2L^{-2})$, are somewhat different from those in metallic mixed-valence Ce systems: In $CePd_3$, $E'(4f^0 \rightarrow 4f^1L^{-1}) \sim -10$ eV,[32,33] as compared to $\sim -14$ eV in $CeO_2$. This would largely be due to efficient screening of the core hole in metallic systems. On the other hand, in the $L_{\rm III}$ x-ray absorption edge of $CeO_2$, two features, probably corresponding to the $4f^0$ and $4f^1L^{-1}$ final states, are separated by only $\sim 10$ eV.[9-11,34] As the final state of the x-ray absorption edge is the same as that of XPS except for the presence of an excited $5d$ electron just above $E_F$, the smaller separation in the x-ray absorption edge may be ascribed to screening of the core hole by the excited electron. Such a difference between XPS and x-ray absorption is expected to be small for metallic systems, and in fact the same $4f^0$-$4f^1$ separation has been observed for $CePd_3$ (Ref. 11) in XPS and x-ray absorption. The positive value of $E'(4f^1L^{-1} \rightarrow 4f^2L^{-2}) \sim 1.1$ eV is due to a higher Ce $4f^2$ level in $CeO_2$ as compared to trivalent compounds where $E'(4f^1L^{-1} \rightarrow 4f^2L^{-2})$ is negative and the $4f^2$ satellites are due to shake-down transitions. A main discrepancy between the calculated and experimental spectra is the width of the $4f^2$ signal. [In a deconvoluted spectrum in Ref. 16, the $4f^2$ signal is resolved into two peaks, $u''$ and $u'$ ($v''$ and $v'$), though not very clearly.] This is probably due to multiplet splittings of the $3d^94f^2$ final state,[35] which is significant but is neglected in the present calculation.

Our conclusion that $CeO_2$ has $\sim 0.6$ of a $4f$ electron appears to conflict with the simple $4d^94f^1$-like multiplet structures observed in the $4d \rightarrow 4f$ photon absorption.[35,36] Multiplet structures of the $4f^94f^2$ final state clearly seen in $\gamma$-Ce and $4f^1$ compounds become broad and weak, and $4d^94f^1$-like features develop in going to mixed-valence or tetravalent Ce.[12,14] This, however, does not necessarily mean that $CeO_2$ is mainly $4f^0$, because the $4d^94f^2$ multiplet structures could disappear not only by complete absence of the $4f$ electron but also by absence of certain orbital components of Ce $4f$: In the ground state of $CeO_2$ there is essentially only $4f$ $a_{2u}$ electrons (Table I), and therefore the final state is $4d^94f^1+4f^94f(a_{2u})^14f^1$. The multiplicity of the $4d^94f(a_{2u})^14f^1$ configuration is only twice that of $4d^94f^1$ resulting in the structure as simple as $4d^94f^1$. As for $\alpha$-Ce, which will be discussed in Sec. VI, although the local symmetry of the $4f^1$ configuration is the same as $CeO_2$, other components of Ce $4f$, $t_{2u}$, and/or $t_{1u}$ would be also present and more complete $4d^94f^2$ features have been observed.[6] Thus we think that the $4d \rightarrow 4f$ absorption structure cannot be used directly as a tool for monitoring the $4f$ occupancy.

## V. CeN

CeN is a mixed-valence material, where $4f^05d^n \leftrightarrow 4f^15d^{n-1}$ configuration mixing is thought to give rise to anomalous magnetism and lattice volume[22] [$6s$ is omitted in $(5d\,6s)^n$ as the Ce $6s$ states in CeN are well above the Ce $5d$ states]. However, as can be seen from the $CeO_2$ results, it would be important to consider also the local configuration mixing $4f^0 \leftrightarrow 4f^1L^{-1}$ ($5d^n$ is omitted for brevity) in CeN, as it has an electronic structure similar to that of $CeO_2$ with the closed N $2p$ shell apart from the presence of the $5d$ conduction electrons. In order to assess the importance of the $4f^0 \leftrightarrow 4f^1L^{-1}$ mixing, we try to explain the core-level XPS (Ref. 25) and resonant photoemission[26] spectra by taking into account only the $4f$-$L$ mixing and by neglecting effects of $5d$ conduction electrons. (Note that the $4f$-$5d$ mixing on a single Ce atom is not allowed by symmetry.) We consider the Ce $4f$ and N $2p$ orbitals in the $CeN_6^{12-}$ cluster and $l = t_{1u}$ and $t_{2u}$ in Eq. (3). $V_1$ and $V_2$ are obtained by assuming $(fp\sigma) = -2(fp\pi) = 0.4$ eV, which is a little smaller than that for La pnictides [$(fp\sigma) = 0.5$ eV] used in Ref. 37. Thus we use $V_1 = 1.38$ eV and $V_2 = -0.98$ eV. In (13) $\bar{V}_1 = V_2$ and $\bar{V}_2 = \sqrt{5/6}V_2$ for the $t_{1u}$-like hole and $\bar{V}_1 = \sqrt{5/6}V_1$ and $\bar{V}_2 = V_2$ for the $t_{2u}$-like hole.

The XPS spectrum of the Ce $3d$ core level[25] in Fig. 6 shows $4f^0$ signals as well as the $4f^1$ main lines and the $4f^2$ shake-down satellites, which is characteristic of mixed valency. The valence-band photoemission spectra for photon energy just below and on the $4d \rightarrow 4f$ resonance[26] are also shown in the figure and the difference between the two spectra may be thought of as the $4f$-derived emission. In the original assignment[26] the splitting of the peaks $A$ and $B$ ($C$ and $D$) has been attributed to surface effects: $B(D)$ has been attributed to emission from the surface-stabilized $4f^1$ initial state.

The $3d$ core-level spectrum has been reproduced with the use of parameters $E_0 = -1.6$, $E_1 = -11.4$, and $E_2 = -4.0$ eV as shown in Fig. 6. The $4f$ occupancy is thus given to be $\sim 0.8$. The $4f$ spectra calculated with the above $E_0$, $E_1$, and $E_2$ and $\epsilon_L = -2.2$ eV are shown as a function of $E_a$ in Fig. 7, where as in the case of $CeO_2$ stronger and weaker lines are, respectively, the main $4f$ lines and the $L \rightarrow 4f$ satellites. The $4f$ spectrum with $E_a = 1.4$ eV seems to reproduce well the three peaks $B$, $C$, and $D$ and is superposed in Fig. 6. The peak $A$ is not reproduced in the calculated spectrum and would be due to mixing of $4f$ into the $5d$ conduction band which has

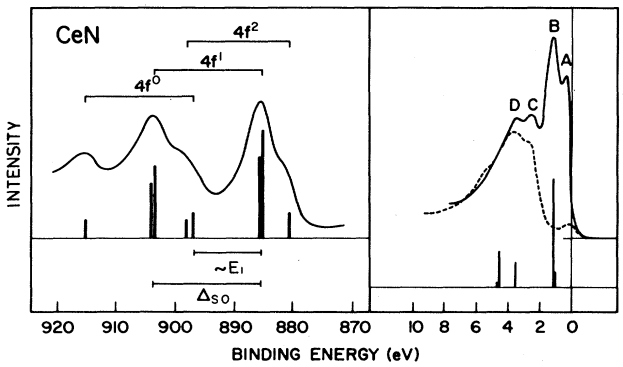


FIG. 6. Experimental (Refs. 25 and 26) and calculated Ce $3d$ core-level x-ray photoemission (left-hand side) and valence-band photoemission (right-hand side) spectra of CeN. Valence-band spectra for photon energies just below and on the $4d \rightarrow 4f$ resonance are given by dashed and solid curves, respectively. Calculated spectra are indicated by vertical bars. $E_1 = E'(4f^0 \rightarrow 5f^1 L^{-1})$. $\Delta_{so}$ is the spin-orbit splitting of Ce $3d$. The calculated $4f$-derived spectrum is that for $E(4f^0 L^{-1} \rightarrow 4f^1 L^{-2}) = 1.4$ eV and $\epsilon_L = -2.2$ eV.

not been included in our model. Surface states have not been completely ruled out, however, as we could identify the peaks $A$, $C$, and $D$ with the bulk emission and the peak $B$ with the surface $4f$ level which is not visible in the XPS valence-band spectrum[25] due to the low surface sensitivity of XPS. In this case, the $4f$-$5d$ hybridized band may not be enhanced very much or may overlap the peak $A$ or $B$.

The nonmagnetic properties and the small lattice volume of CeN can be understood within the present mixed-valence description by an analogy to $CeO_2$. The Curie-Weiss behavior at high temperatures[22] would be due to localized $4f^1$ excited states, which may be located closely to the ground state due to $4f$-$5d$ interactions. In the $4f^0 \leftrightarrow 4f^1 L^{-1}$ mixing, the number of conduction electrons is one per Ce atom. The conduction-electron number obtained from the optical measurement[27] is a little smaller than this, but we note that this number has been obtained by assuming an effective mass of the $5d$ band and is dependent on the assumed mass. Depopulation of the conduction band at high temperatures has been observed in this optical study,[27] which is consistent with our model where localized $4f^1$ states are thermally populated, resulting in the reduced conduction-electron number.

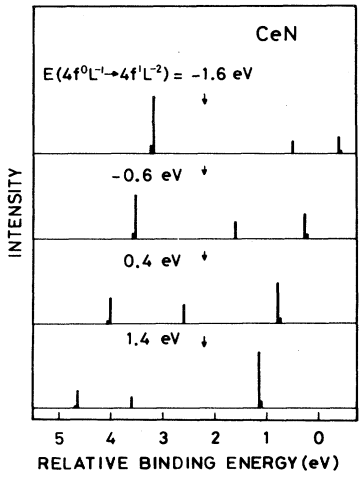


FIG. 7. Calculated $4f$-derived photoemission spectra of CeN as a function of $E_a = E(4f^0 L^{-1} \rightarrow 4f^1 L^{-2})$. The N $2p$ ($t_{1u}$ and $t_{2u}$) level (equal to $\epsilon_L$) is shown by arrows.

Thus the satellite features in the $4f$-derived spectrum of CeN are explained by the $4f^0 \leftrightarrow 4f^1 L^{-1}$ mixing. However, the ground-state parameter $E_0 = E(4f^0 \rightarrow 4f^1 L^{-1}) = -1.6$ eV may be inconsistent with the parameter $E_a = E(4f^0 L^{-1} \rightarrow 4f^1 L^{-2}) = 1.4$ eV in the valence-hole state, since $E_a$ and $E_0$ should not differ by more than a Coulomb energy between two $L$ holes, which would be at most $\sim 1$ eV. Here we note that the calculated $4f$ spectrum is not sensitive to $E_0$ (the spectral line positions were independent on $E_0$ and the intensities did not change very much with $E_0$ up to $E_0 \sim 1.5$ eV), and therefore the higher $E_0$ would be more appropriate. The higher $E_0$, however, would lead to too large $I_{4f^0}/I_{4f^1}$ core-level intensity ratio, and the extended $4f^0 5d^n \leftrightarrow 4f^1 5d^{n-1}$ process in addition to the local $4f^0 \leftrightarrow 4f^1 L^{-1}$ one should be considered in order to give the intense $4f^1$ core-level lines and consequently the large $4f^1$ component in the ground state. The present model could in principle be extended to include the two valence-mixing mechanisms by the use of a large cluster. Such a study would reveal relative importance of the two valence-mixing processes and also make unambiguous assignment of the $4f$-derived spectrum in CeN.

## VI. $\gamma$-to-$\alpha$ PHASE TRANSITION OF Ce METAL

So far several models have been proposed for the $\gamma$-to-$\alpha$ transition of the Ce metal: (i) promotion of the $4f$ electrons to the $5d\,6s$ conduction band in going from the $\gamma$-to-$\alpha$ phase,[38] that is, Ce changes from trivalent ($4f^1$) to tetravalent ($4f^0$), (ii) a Mott transition within the $4f$ band,[39] (iii) an increase of the $5d\,6s$-$4f$ hybridization in the $\alpha$ phase,[40] and (iv) a Kondo model, according to which the $\alpha$ phase is identified as a Kondo singlet state.[41,42] The promotion model is in contradiction to the almost unchanged $4f$ number across the transition revealed by positron annihilation,[2] Compton scattering,[3] photoemission spectroscopy,[4–6] and energy-band calculations,[7,8,40] and also has been criticized by a thermodynamical argument.[3] The Mott transition assumes the constant $4f$ number but the width of the $4f$ band $W$ is of the order of 1 eV,[7,8,40] while the Coulomb repulsion between two $4f$ electrons on one atom is $U \sim 5$ eV,[43] which does not satisfy the condition $W \sim U$ for a Mott transition to occur. The Kondo model,[41,42] on the other hand, is successful in explaining the disappearance of the magnetic moment and the volume collapse in the $\gamma$-to-$\alpha$ transition.

Here we would like to describe this transition as a change in the local electronic configuration of the $4f$ level: Nonmagnetic but essentially $4f^1$-like $\alpha$-Ce is described by the ground state of the forms (3) and (4). In the case of Ce metal, the smallest cluster relevant to the problem is $Ce_{13}$, where the $4f$ orbitals on the central atom and the $5d\,6s$ orbitals on the 12 nearest-neighbor Ce atoms are considered. This is already considerably complicated as

compared to the $CeO_8$- or $CeN_6$-cluster problem, and we give here only qualitative discussions using a simplified model. The ground state of $\gamma$-Ce may be described as

$$\Psi_\gamma = f^\dagger | 0 \rangle , \tag{15}$$

where $f^\dagger$ creates an electron in the $^2F_{5/2}$ state of the Ce $4f^1$ ion. For $\alpha$-Ce,

$$\Psi_\alpha = c_0 | 0^* \rangle + \sum_l c_l | l^* \rangle , \tag{16}$$

$$| l^* \rangle = \sum_{i,j} \Gamma^l_{ij} \sum_\sigma f^\dagger_{i\sigma} d_{j\sigma} | 0^* \rangle , \tag{17}$$

analogous to Eqs. (3) and (4). Here $| 0^* \rangle$ is different from $| 0 \rangle$ in that there is one more non-$4f$ electron in $\alpha$-Ce added near $E_F$ per Ce atom as compared to $\gamma$-Ce. $d_{i\sigma}$ annihilates a $5d\,6s$ electron on the nearest-neighbor atoms of the central $4f$ ion. For $\alpha$-Ce we expect $| c_0 | \gg | c_l |$, that is, the $4f$ occupancy is close to 1. The energies of the $\gamma$ and $\alpha$ phases may be roughly estimated as follows: for the $\gamma$ phase,

$$E_\gamma = E(4f^1) , \tag{18}$$

for the $\alpha$ phase, two configurations, $4f^1 5d^{-1}\epsilon_F$ and $4f^0\epsilon_F$, where $\epsilon_F$ stands for an extra electron added near $E_F$. For simplicity we consider only one state for each configuration. Then the energy of the $\alpha$ phase is given by

$$E_\alpha = \{E_A + E_B - [(E_A - E_B)^2 + 4V^2]^{1/2}\}/2 , \tag{19}$$

where $E_A = E(4f^1 5d^{-1}\epsilon_F)$, $E_B = E(4f^0\epsilon_F)$, and $V$ is the matrix element of the Hamiltonian between the two states.

In Fig. 8 we present, according to (18) and (19), the free energy $H = E - TS$ per Ce atom for $\gamma$- and $\alpha$-Ce as a function of the Ce-Ce interatomic distance at room temperature. The local symmetry of the magnetic $4f^1$ configuration in $\gamma$-Ce is $^2F_{5/2}$, while the $4f^0\epsilon_F$ and $4f^1 5d^{-1}\epsilon_F$ configurations have the $^1S_0$ (or $^1A_{1g}$) local symmetry and

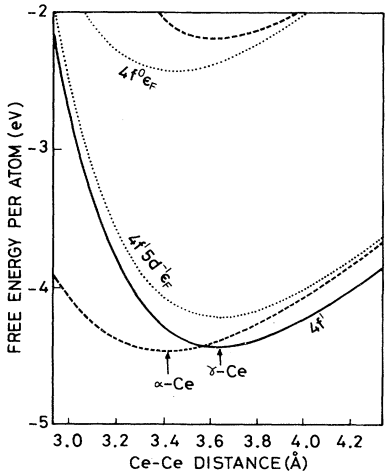


FIG. 8. Free energies $E - TS$ of $\alpha$- and $\gamma$-Ce at room temperature as a function of the nearest-neighbor Ce-Ce distance. The $4f^1$ configuration (solid curve) corresponds to $\gamma$-Ce, and the bonding state (lower dashed curve) of the $4f^0\epsilon_F$ and $4f^1 5d^{-1}c_F$ configurations (dotted curves) corresponds to $\alpha$-Ce. The equilibrium distances for $\alpha$- and $\gamma$-Ce are shown by arrows.

are mixed with each other via $V$. $V$ increases rapidly as the lattice parameter decreases. The energies of $4f^1$ and $4f^1 5d^{-1}\epsilon_F$ are expected to have nearly the same lattice parameter dependence due to similar configurations with one $4f$. The $4f^0\epsilon_F$ energy is higher than $4f^1$ or $4f^1 5d^{-1}\epsilon_F$ by the $4f \rightarrow 5d\,6s$ promotion energy ($\sim 2$ eV) and has a minimum for a lattice parameter smaller than the $4f^1$ configurations. The $4f^1 5d^{-1}\epsilon_F$ energy is lowered by forming a $5d$–$4f$ bond through $V$ according to Eq. (19) as is shown in Fig. 8, and produces a minimum at a smaller lattice volume, which we identify as the $\alpha$ phase. In the figure we also present an antibonding counterpart of the bonding $4f^1 5d^{-1}\epsilon_F + 4f^0\epsilon_F$ state. One can see that $\alpha$-Ce is almost $4f^1 5d^{-1}\epsilon_F$-like, and therefore the $4f$ occupancy is close to unity (in this simplified model the $4f$ number is calculated to be $\sim 0.9$). The $\gamma$-to-$\alpha$ transition is thus clearly a first-order phase transition accompanied by a change in the symmetry of electronic state and by a volume collapse. We have assumed volume dependence of the energies of the unhybridized configurations and $V$ as

$$E(4f^1) = 4.43[(3.64/d)^{5.06} - 2(3.64/d)^{2.53}] , \tag{20}$$

$$E(4f^1 5d^{-1}\epsilon_F) = E(4f^1) + a , \tag{21}$$

$$E(4f^0\epsilon_F) = 4.43\{[3.64/(d+0.2)]^{5.06} - 2[3.64/(d+0.2)]^{2.53}\} + b , \tag{22}$$

$$V = V_0(3.64/d)^6 , \tag{23}$$

where the Ce-Ce distance $d$ is in Å and energies in eV. The exponents, prefactors, etc., in Eqs. (20)–(22) are so chosen as to give the elastic constant, cohesive energy, and equilibrium lattice parameter of the $\gamma$ phase. The $d^{-6}$ law of $V$ is due to the interatomic distance dependence of the $d$-$f$ transfer integrals.[44] We have chosen the parameters in Eqs. (21)–(23) as $V_0 = 0.6$, $a = 0.22$, and $b = 2$ eV, so that the $\alpha$ phase is more stable by $\sim 1$ kcal (Ref. 45) with the lattice parameter smaller by $\sim 0.2$ Å than the $\alpha$ phase. As the temperature is lowered, the $4f^1$ free energy rises owing to the entropy term $TS$ ($S = k \ln 6$ for $\gamma$-Ce with a $J = \frac{5}{2}$ magnetic moment and $S \sim 0$ for $\alpha$-Ce) and only the $\alpha$ phase is realized, which agrees with the phase diagram of Ce metal.[39]

Resonant photoemission from the $4f$ level[4–6] has shown two peaks (near $E_F$ and at $\sim 2$ eV) and their relative intensity changes across the $\gamma$-to-$\alpha$ transition. In the case of the localized $4f^1$ state ($\gamma$-Ce), resonant photoemission takes place via process $4d^{10}4f^1 + h\nu \rightarrow 4d^9 4f^2 \rightarrow 4d^{10}4f^0 + \epsilon l$ followed by a satellite transition from the $4f^0$-hole to a ligand- or $5d$-hole state. For the mixed-valence case ($\alpha$-Ce),

$$(4d^{10}4f^0\epsilon_F + 4d^{10}4f^1 5d^{-1}\epsilon_F) + h\nu \rightarrow 4d^9 4f^1\epsilon_F + 4d^9 4f^2 5d^{-1}\epsilon_F ,$$

then only the $4f^2$ part leads to a SCK decay

$$4d^9 4f^2 5d^{-1} \rightarrow 4d^{10}4f^0 5d^{-1}\epsilon_F + \epsilon l .$$

For Ce metal, where the ligand level Ce $5d$ is not in a closed-shell configuration as the O $2p$ (N $2p$) levels in $CeO_2$ (CeN), the above two cases make little difference,

and the model for the $4f$-derived photoemission presented in I may be applicable. According to this, the resonant photoemission spectra of $\gamma$- and $\alpha$-Ce may be described as follows: The energy separation of the two $4f$ peaks is given by $(\Delta E^2+4V^2)^{1/2}$, where $\Delta E=E(4f^0\rightarrow 4f^1 5d^{-1})$ for $\gamma$-Ce and $\Delta E=E(4f^0 5d^{-1}\epsilon_F\rightarrow 4f^1 5d^{-2}\epsilon_F)$ for $\alpha$-Ce. As $E(4f^0\epsilon_F\rightarrow 4f^1 5d^{-1}\epsilon_F)\sim -2$ eV in the ground state, we estimate $E(4f^0\rightarrow 4f^1 5d^{-1})\sim -2$ eV whose absolute value is larger than $V$, which explains why the 2-eV emission is stronger than the emission just below $E_F$ in $\gamma$-Ce. On going from $\gamma$- to $\alpha$-Ce, $V$ increases according to (23), which results in an increase of the $E_F$-peak intensity with little change in the separation of the two peaks.

The present model for the $4f$ satellites is similar to a conceptual model by Hüfner and Steiner[46] or a model Hamiltonian study by Gunnarson and Schönhammer[47] in that the screening of the $4f^0$ hole takes place by the $4f$ electron. A recent model proposed by Liu and Ho[48] explains the $4f$ satellites in terms of the screening of the $4f^0$ hole by the $5d$ conduction electron. According to these authors, a localized $5d$ state splits off from the $5d\,6s$ band due to the attractive potential of the $4f^0$ hole, which is either filled or empty in the final state giving rise to the two peaks. However, no such localized state is expected as can be seen from the core-level XPS spectra, where the core hole is screened by the $5d\,6s$ electron in the poorly screened peak and by the $4f$ electron in the well-screened peak, and no splitting into $5d\,6s$-screened and -unscreened peaks is observed, as would be expected from the model of Liu and Ho.

Finally, we compare our $\alpha$-to-$\gamma$ transition model with other models. The promotion model[38] is evidently incompatible with our model, since we have shown that the $4f$ occupancy is close to unity for $\alpha$-Ce. The Mott transition is also not compatible with our model as the $4f$-$5d\,6s$ hybridization $V$ is of the order of $\sim 1$ eV, which may be sufficiently large to stabilize the nonmagnetic configuration, but is far too small to form an itinerant $4f$ band since $V\sim W\ll U$. As has been pointed out by the band calculations,[7,8,40] the $4f$-band width in the collapsed $\alpha$ phase of Ce or tetravalent Ce compounds is significantly increased, and in some tetravalent compounds possibility of the formation of the $4f$ band has been pointed out.[14] It is noted, however, that electrons in such a $4f$ band, if it exists, are strongly correlated and are not appropriately described within a usual one-electron energy-band picture. In the Kondo mechanism[41,42] also, the $4f$-$5d\,6s$ hybridization is essential. The singlet state in $\alpha$-Ce described here may be analogous to the Kondo singlet state. The stabilization mechanism of our singlet state is hybridization between two local configurations $4f^0$ and $4f^1 5d^{-1}$, while in the Kondo model[42] the singlet state is stabilized by the $4f$-$5d\,6s$ exchange interaction which is enhanced in the $\alpha$ phase by increased hybridization. Thus similar pictures seem to have emerged from the two quite different approaches. We note, however, a basic difference between the two approaches is that, in the Kondo model interactions of the $4f$ level with conduction electrons, particularly near $E_F$, are important while in our model interactions with localized (and , for $CeO_2$ and CeN, closed-shell) orbitals are considered. Therefore, the DOS at $E_F$ which is an important parameter in the Kondo model does not enter our model, which might explain dense Kondo behaviors, e.g., in $CeB_6$ (Ref. 49), where a magnetic moment is quenched with relatively low concentration of electrons at $E_F$. A drawback of our model is obviously that it cannot treat properly itinerant (e.g., $5d\,6s$) electrons, thus we cannot study their contributions to electrical conduction, specific heats, etc., whereas it describes local correlation effects of the $4f$ ions in a realistic way.

## VII. DISCUSSION

Generally in metallic mixed-valence Ce systems, the two configurations $4f^0(5d\,6s)^n$ and $4f^1(5d\,6s)^{n-1}$ have been thought to be degenerate. The present local mechanism $4f^0\rightarrow 4f^1 L^{-1}$ explains mixed valency in insulating compounds and also part of valence mixing in metallic compounds. This results from the large $4f$-$L$ hybridization in Ce compounds, where the $4f$ orbital is the most extended in the rare-earth series. Importance of the $p$-$f$ mixing, where $p$ corresponds to $L$ here, as compared to the $f$-$d$ mixing in stable-valence Ce pnictides has been pointed out by Kasuya and co-workers.[37,50] In the $4f^0\leftrightarrow 4f^1 L^{-1}$ valence-mixing mechanism strong hybridization between $4f$ and localized orbital $L$ quenches the magnetic moment. In the $4f^0(5d\,6s)^n\leftrightarrow 4f^1(5d\,6s)^{n-1}$ mixing, on the other hand, each matrix element for the $4f$-$5d$ mixing may be small, but interactions involving conduction-band levels near $E_F$ need only low virtual excitation energies and therefore can be significant. In the case of metallic systems such as $CePd_3$, $\alpha$-Ce, etc., we cannot separate unambiguously the two mechanisms, since the energy band formed by orbitals on neighboring atoms crosses $E_F$ and shows either localized or extended characters. The local $4f^0\leftrightarrow 4f^1 L^{-1}$ process would particularly be important in the case of a narrow $L$ band, particularly a closed-shell $L$ band, as interatomic Coulomb interactions lower the energy of a localized electron-hole pair $4f^1 L^{-1}$ as compared to a well-separated pair. This interatomic Coulomb energy has not been incorporated in theories which use Anderson Hamiltonians.[24,41,42,47,51]

In the present paper we have treated electron correlations within the small cluster. This is a good approximation for localized excitations, namely core-hole states, $4f$-hole states, etc., but might not be a good approximation for the ground state where equivalent rare-earth ions interact with each other. It is considerably difficult to treat correlation effects in a large system, however. On the other hand, there are a number of experiments showing that a single rare-earth ion exhibits mixed-valence behavior in a dilute system.[52,53] This fact means that the valence mixing is essentially of the single-ion nature and that the present model which uses the small clusters is relevant to the valence-mixing phenomena.

Although the one-electron theory such as energy-band calculations and molecular-orbital calculations can predict certain ground-state properties of narrow band systems such as Ce compounds, physical properties associated with excited states have to be treated beyond the one-electron picture. This is most clearly seen in Fig. 5, where the $4f$-derived photoemission spectra are distributed in a

wider energy range than the initial-state one-electron Ce $4f$-like partial DOS. This can be understood as follows: While in the molecular-orbital levels Ce $4f$ have a width of the order of the Ce $4f$—O $2p$ transfer integral $W$, the Ce $4f$ photoemission has a width of $\sim n^{1/2}W$, where $n$ is the number of overlapping Ce $4f$—O $2p$ pairs per Ce ion, including spin degeneracy. Thus information obtained by resonant photoemission is preferentially for local electronic structure of the Ce ion rather than for, if it exists, extended band states.

This local electronic structure is directly related to the $4f^0$-hole state produced by the SCK decay of the $4d^9 4f^2$ state ($4d^9 4f^2 \rightarrow 4d^{10} 4f^0$) followed by satellite transitions, e.g., $L \rightarrow 4f$. A sum rule

$$\epsilon_{4f} = \int A_{4f}(\epsilon)\epsilon \, d\epsilon \tag{24}$$

gives the pure $4f^0$-hole energy $\epsilon_{4f}$ in analogy to the sum rule for the core-level photoionization.[54] Here $A_{4f}(\epsilon)$ is the $4f$ spectral density which is the difference between the spectral intensity at the $4d \rightarrow 4f$ resonance and that at the antiresonance. Equation (24) combined with the resonant photoemission spectra[4–6] suggests that in $\gamma$- and $\alpha$-Ce $\epsilon_{4f}$ is 1—2 eV below $E_F$, with a slight shift to lower binding energies in going from $\gamma$-Ce to $\alpha$-Ce. For trivalent $4f^1$ compounds as was studied in I, the $4f$ energy thus obtained bears connection to the ground-state $4f$ level. But in mixed-valence systems $\epsilon_{4f}$ is the energy of a localized $4f^0$ hole and it is not straightforward to relate $\epsilon_{4f}$ with a ground-state energy level.

In the mixed-valence system the $4f$ character might be present in delocalized (bandlike) states via hybridization between $4f$ and delocalized states. One-electron $4f$-like partial DOS as obtained by band calculations might have some relevance to this $4f$ character, except for the high-$4f$ DOS region.[55] For $4f$-band states, one would expect to observe valence-band satellites as in Ni, namely localized and itinerant $4f$ holes.[56,57] If this is the case, quite different resonant enhancement as a function of photon energy is expected for the two types of hole states, since resonance photoemission enhances localized final states selectively. [In localized $4f^1$ Ce pnictides (I), the same enhancement has been observed for resonant ($h\nu \sim 120$ eV) and nonresonant ($h\nu \sim 50$ eV) (Ref. 58) spectra, which is consistent with the $4f$ hole localized on one Ce ion.] On the other hand, we note that in either case of the localized, mixed-valence and bandlike $4f$ states, intensities of core levels ($4f^0$, $4f^1$, and $4f^2$) are expected to give useful quantitative information on the $4f$ number in the initial ground state, as the strong core-hole potential causes localization of the $4f$ electrons.

## ACKNOWLEDGMENTS

The author would like to thank L. Schlapbach and H. C. Siegmann for their interest and encouragement in this work. This work was partly supported by the Swiss National Energy Research Fund.

*Present address.

[1] D. C. Koskenmaki and K. A. Gschneidner, Jr., in *Handbook of the Physics and Chemistry of the Rare Earths,* edited by K. A. Gschneidner, Jr., and L. Eyring (North-Holland, Amsterdam, 1978), Vol. 1, p. 337; J. M. Lawrence, P. S. Riseborough, and R. D. Parks, Rep. Prog. Phys. 44, 1 (1981).

[2] D. R. Gustafson, J. O. McNutt, and L. O. Roelling, Phys. Rev. 183, 435 (1969).

[3] U. Kornstädt, R. Lässer, and B. Lengeler, Phys. Rev. B 21, 1898 (1980).

[4] N. Mårtensson, B. Reihl, and R. D. Parks, Solid State Commun. 41, 573 (1982).

[5] R. D. Parks, N. Mårtensson, and B. Reihl, in *Valence Instabilities,* edited by P. Wachter and H. Boppart (North-Holland, Amsterdam, 1982), p. 239.

[6] D. Wieliczka, J. H. Weaver. D. W. Lynch, and C. G. Olson, Phys. Rev. B 26, 7056 (1982).

[7] D. Glötzel and L. Fritsche, Phys. Status Solidi B 79, 85 (1977).

[8] W. E. Pickett, A. J. Freeman, and D. D. Koelling, Phys. Rev. B 23, 1266 (1981).

[9] K. R. Bauchspiess, W. Boksch, E. Holland-Moritz, H. Launois, R. Pott, and D. Wohlleben, in *Valence Fluctuations in Solids,* edited by L. M. Falicov, W. Hanke, and M. B. Maple (North-Holland, Amsterdam, 1981), p. 417.

[10] G. Krill, J. P. Kappler, A. Meyer, L. Abadli, and M. F. Ravet, J. Phys. F 11, 1713 (1981).

[11] A. Bianconi, M. Campagna, and S. Stizza, Phys. Rev. B 25, 2477 (1982).

[12] D. J. Peterman, J. H. Weaver, and M. Croft, Phys. Rev. B 25, 5530 (1982).

[13] J. W. Allen, S.-J. Oh, I. Lindau, M. B. Maple, J. F. Suassuna, and S. B. Hagström, Phys. Rev. B 26, 445 (1982).

[14] D. J. Peterman, J. H. Weaver, M. Croft, and D. T. Peterson, Phys. Rev. B 27, 808 (1983).

[15] P. Wachter, in *Valence Instabilities,* Ref. 5, p. 145.

[16] P. Burroughs, A. Hamnett, A. F. Orchard, and G. Thornton, J. Chem. Soc. Dalton Trans. 1976, 1686.

[17] A. Fujimori, Phys. Rev. B 27, 3992 (1983).

[18] G. Thornton and M. J. Dempsey, Chem. Phys. Lett. 77, 409 (1981).

[19] D. D. Koelling, Solid State Commun. 43, 247 (1982).

[20] J. W. Allen, S.-J. Oh, I. Lindau, J. M. Lawrence, L. I. Lindau, L. I. Johansson, and S. B. Hagström, Phys. Rev. Lett. 46, 1100 (1981).

[21] M. Croft, J. H. Weaver, D. J. Peterman, and A. Franciosi, Phys. Rev. Lett. 46, 1104 (1981).

[22] J. Danan, C. de Novion, and R. Lallement, Solid State Commun. 7, 1103 (1969).

[23] W. E. Gardner, J. Penfold, T. F. Smith, and I. R. Harris, J. Phys. F 2, 133 (1972).

[24] H. A. Razafimandimby and P. Erdös, Z. Phys. B 46, 193 (1982).

[25] Y. Baer and Ch. Zürcher, Phys. Rev. Lett. 39, 956 (1977).

[26] W. Gudat, R. Rosei, J. H. Weaver, E. Kaldis, and F. Hulliger, Solid State Commun. 41, 37 (1982).

[27] A. Schlegel, E. Kaldis, P. Wachter, and Ch. Zürcher, Phys.

Lett. 66A, 125 (1978).
[28]R. A. Pollack, S. P. Kowalczyk, and R. W. Johnson, in *Valence Instabilities and Related Narrow Band Phenomena,* edited by R. D. Parks (Plenum, New York, 1977), p. 463.
[29]A. Fujimori, Phys. Rev. B (in press).
[30]A. F. Orchard and G. Thornton, J. Electron Spectrosc. Relat. Phenom. 10, 1 (1977).
[31]E. Umbach, Surf. Sci. 117, 482 (1982).
[32]R. Lässer, J. C. Fuggle, M. Beyss, M. Campagna, F. Steglich, and F. Hulliger, Physica 102B, 360 (1980).
[33]F. U. Hillebrecht and J. C. Fuggle, Phys. Rev. B 25, 3550 (1982).
[34]P. R. Sarode, D. D. Sarma, R. Vijayaraghavan, S. K. Malik, and C. N. R. Rao, J. Phys. C 15, 6655 (1982).
[35]R. Haensel, P. Rabe, and B. Sonntag, Solid State Commun. 8, 1845 (1970).
[36]B. E. Koel, G. M. Loubriel, M. L. Knotek, R. H. Stulen, R. Rosenberg, and C. C. Parks, Phys. Rev. B 25, 5551 (1982).
[37]H. Takahashi, K. Takegahara, A. Yanase, and T. Kasuya, in *Valence Instabilities,* Ref. 5, p. 379.
[38]R. Ramirez and L. M. Falicov, Phys. Rev. B 3, 2425 (1971); B. Coblin and A. Blandin, Adv. Phys. 17, 281 (1968).
[39]B. Johansson, Philos. Mag. 30, 469 (1974); A. Platau and S.-E. Karlsson, Phys. Rev. B 18, 3820 (1978).
[40]H. H. Hill and E. A. Kmetko, J. Phys. 5, 1119 (1975).
[41]M. Lavagna, C. Lacroix, and M. Cyrot, Phys. Lett. 90A, 210 (1982).
[42]J. W. Allen and R. M. Martin, Phys. Rev. Lett. 49, 1106 (1982).
[43]J. K. Lang, Y. Baer, and P. A. Cox, Phys. Rev. Lett. 42, 74 (1979); J. Phys. F 11, 121 (1981).
[44]W. A. Harrison, *Electronic Structure and the Properties of Solids* (Freeman, San Francisco, 1980).
[45]R. I. Beecroft and C. A. Swenson, J. Phys. Chem. Solids 15, 234 (1960).
[46]S. Hüfner and P. Steiner, Z. Phys. B 46, 37 (1982); in *Valence Instabilities,* Ref. 5, p. 263.
[47]O. Gunnarson and K. Schönhammer, Phys. Rev. Lett. 50, 604 (1983).
[48]S. H. Liu, and K.-M. Ho, Phys. Rev. B 26, 7052 (1982).
[49]K. Samwer and K. Winzer, Z. Phys. B 25, 269 (1976).
[50]T. Kasuya, IBM J. Res. Dev. 14, 214 (1970); J. Phys. (Paris) 37, C4-261 (1976).
[51]L. M. Falicov and J. C. Kimball, Phys. Rev. Lett. 22, 997 (1969); R. Ramirez, L. M. Falicov, and J. C. Kimball, Phys. Rev. B 2, 997 (1969).
[52]J. S. Schilling, Adv. Phys. 28, 657 (1980).
[53]T. M. Holden, W. J. L. Buyers, P. Martel, M. B. Maple, and M. Tovar, in *Valence Instabilities,* Ref. 5, p. 325.
[54]B. I. Lundqvist, Phys. Kondens. Mater. 9, 236 (1969).
[55]A. Yanase, J. Magn. Magn. Mater. 31-34, 453 (1983).
[56]S. Hüfner and G. K. Wertheim, Phys. Lett. 51A, 299 (1975); C. Guillot, Y. Ballu, J. Paigué, J. Lecante, K. P. Jain, P. Thiry, R. Pinchaux, Y. Pétroff, and L. M. Falicov, Phys. Rev. Lett. 39, 1632 (1977).
[57]D. R. Penn, Phys. Rev. Lett. 42, 921 (1979); A. Liebsch, *ibid.* 43, 1431 (1979).
[58]A. Franciosi, J. H. Weaver, N. Mårtensson, and M. Croft, Phys. Rev. B 24, 3651 (1981).